

Supplementary Information

Aldol condensation of biomass-derived platform molecules over amine-grafted hierarchical FAU nanosheets (Zeolean) featuring basic sites

Thittaya Yutthalekha,^a Duangkamon Suttipat,^a Saros Salakhum,^a Anawat Thivasasith,^a Somkiat Nokbin,^b Jumras Limtrakul,^c and Chularat Wattanakit^{a*}

^a Department of Chemical and Biomolecular Engineering, School of Energy Science and Engineering, Vidyasirimedhi Institute of Science and Technology, Rayong, 21210, Thailand.

^b Department of Chemistry, NANOTEC Center for Nanoscale Materials Design for Green Nanotechnology, and Center for Advanced Studies in Nanotechnology and Its Applications in Chemical, Food and Agricultural Industries, Faculty of Science, Kasetsart University, Bangkok 10900, Thailand.

^c Department of Materials Science and Engineering, School of Molecular Science and Engineering, Vidyasirimedhi Institute of Science and Technology, Rayong 21210, Thailand

* Corresponding author; e-mail chularat.w@vistec.ac.th

Experimental details

Materials. Sodium aluminate (NaAlO_2 : 56 wt% Al_2O_3 and 44 wt% Na_2O , Riedel-de Haën), sodium silicate ($\text{Na}_2\text{Si}_3\text{O}_7$: 26.5 wt% SiO_2 and 10.6 wt% Na_2O , Merck), sodium hydroxide (NaOH : 97%, Carlo Erba) were used as alumina, silica sources and mineralizing agent, respectively. A 3-(trimethoxysilyl) propyl octadecyl-dimethyl-ammonium chloride (TPOAC: 42 wt% in methanol, Aldrich) was used as the structure directing agent (SDA). Sodium chloride (NaCl : 99%, Carlo Erba), calcium chloride (CaCl_2 : 99%, Ajax) and barium chloride (BaCl_2 : 99%, UNIVAR) were used as ion-exchange reagents. A 3-aminopropyl-triethoxysilane (APTES: 97%, Sigma-aldrich) was used as an amine grafting reagent. To study the catalytic aldol condensation, a 5-hydroxymethylfurfural (5-HMF: 99%, Aldrich), acetone (Ac: 99%, Qrec) and decane ($\text{C}_{10}\text{H}_{22}$: 99%, Aldrich) were used as reactant, solvent and internal standard, respectively.

Synthesis of NaX zeolite. Zeolite X was synthesized following a modified literature procedure.¹ The molar composition of the synthesis gel was 3 SiO₂: 3.5 Na₂O: 1 Al₂O₃: 180 H₂O: 0.06 TPOAC. To prepare the synthesis gel, the sodium aluminate solution containing a 1.0 g of NaAlO₂, 0.5 g of NaOH and 3.2 g of DI water was dropwisely added to the sodium silicate solution containing a 3.7 g of Na₂Si₃O₇, 0.2 g of NaOH and 11.2 g of DI water. The obtained mixture was vigorously stirred for 1 h. Subsequently, a 0.4 ml of TPOAC was added as the structure-directing agent (SDA). The gel was aged at room temperature for 24 h and then statically crystallized for 4 days at 75 °C. The synthesized zeolite was collected and washed with DI water until the pH of filtrate less than 8. After drying overnight at 100 °C, the product was calcined in air at 350 °C for 15 h to completely remove the SDA (see Fig. S3). The conventional zeolite X was also prepared using the same procedure, but without the addition of the surfactant.

Preparation of MX zeolite. The ion-exchanged zeolite with alkaline cations were prepared by using 0.1 M MCl₂ solution (M = Ca and Ba). Typically, a 1 g of zeolite powders were treated in 50 ml of MCl₂ solution at room temperature for 6 h. Then, catalysts were separated by filtration and washed with DI water. Finally, the powders were dried in an oven at 110°C. The procedures were repeated until the ion exchange degree (%IED) was approximately 95%.

Grafting of aminosilane molecules on NaX zeolite surfaces. The catalysts were prepared by grafting 3-aminopropyl-triethoxysilane (APTES) molecules on NaX zeolite surfaces. A 2.4 g of zeolite powders were treated in 40 ml of ethanol solution containing a 10 ml of APTES at room temperature for 40 h. The catalysts were recovered by filtration after washing with excess ethanol. Then, the powders were dried in an oven at 110°C. The amine-grafted silica was also prepared with the same procedure.

Characterization. X-ray diffraction (XRD) patterns were collected using a Bruker D8 ADVANCE instrument. The morphology of zeolites was observed by scanning electron microscopy (SEM) performed on a JEOL JSM-7610F microscope with an accelerating voltage of 5 kV and transmission electron microscopy (TEM) performed on a JEOL JEM-2100 microscope at 200 kV. Thermogravimetric analysis (TGA) of as-synthesized zeolite was carried out using Perkin Elmer Pyris 1 TGA instrument in air atmosphere with temperature ramp rate of 10°C.min⁻¹. The infrared spectrum was recorded using a Perkin Elmer Frontier ATR-FTIR spectrometer. The solid-state ¹³C NMR measurements were carried out on a Bruker Ascend 400 MHz

spectrometer. The textural properties of zeolites were analyzed by N₂ adsorption-desorption isotherms using a Belmax apparatus performed at -196 °C. Prior to each measurement, the sample was degassed at 300 °C for 24 h. The specific surface area (S_{BET}) was determined by using the Brunauer–Emmett–Teller (BET) theory. The micropore volume (V_{micro}), the micropore area (S_{micro}) and the external surface area (S_{ext}) were determined by the t -plot method. The total pore volume (V_{total}) was estimated at P/P_0 of 0.99. The elemental data were estimated by X-ray fluorescence (XRF) spectrometry performed on a Bruker AXS S8 Tiger Pioneer instrument. The basicity of catalysts was determined by temperature-programmed desorption of carbon dioxide (CO₂-TPD) performed on a BELCAT II instrument equipped with thermal conductivity detectors (TCD). Prior to the measurement, the catalyst was preheated at 300 °C for 1 h under the flow of He. Then the catalyst was saturated with CO₂ at 100 °C for 30 min and subsequently flushed under the flow of He for 30 min to remove the physically adsorbed CO₂. The TPD profiles were recorded in the temperature range of 100 to 650 °C with the heating rate of 10 °C.min⁻¹.

Catalytic tests. The liquid-phase catalytic aldol condensation of 5-Hydroxymethylfurfural (5-HMF) and acetone (Ac) was performed by using a high pressure compact laboratory reactor (Parr reactor series 5500) equipped with a PID temperature controller and magnetic drive. The reactions were carried out at 130 °C and autogenous pressure. Typically, a 10 ml of 10 wt% of 5-HMF in acetone was added to a 0.5 g of catalysts. At the desired time, the reaction was stopped and products were analyzed by gas chromatography (Agilent 7820B GC) equipped with mass spectrometer (Agilent 5977A MSD) and a HP-5MS column. The conversion was calculated based on the consumption of 5-HMF as the amount of acetone was in an excess. The calibration curve was plotted by using the ratio of the ion abundance (m/z of 67) of the furan fragment ion generated from 5-HMF, which is the same fragment ion found in both reactant and product, to the ion abundance of decane as internal standard (m/z of 57) as shown in Fig. S1. The mass balance was calculated for all experiments in the range of 104±5%. In addition, the mass data corresponding to 4-[5-(hydroxymethyl)furan-2-yl]but-3-en-2-one (m/z = 166, 151, 135, 67, 77, 43) and 4-hydroxy-4-methyl-2-Pentanone (m/z = 101, 59, 43) were also demonstrated.

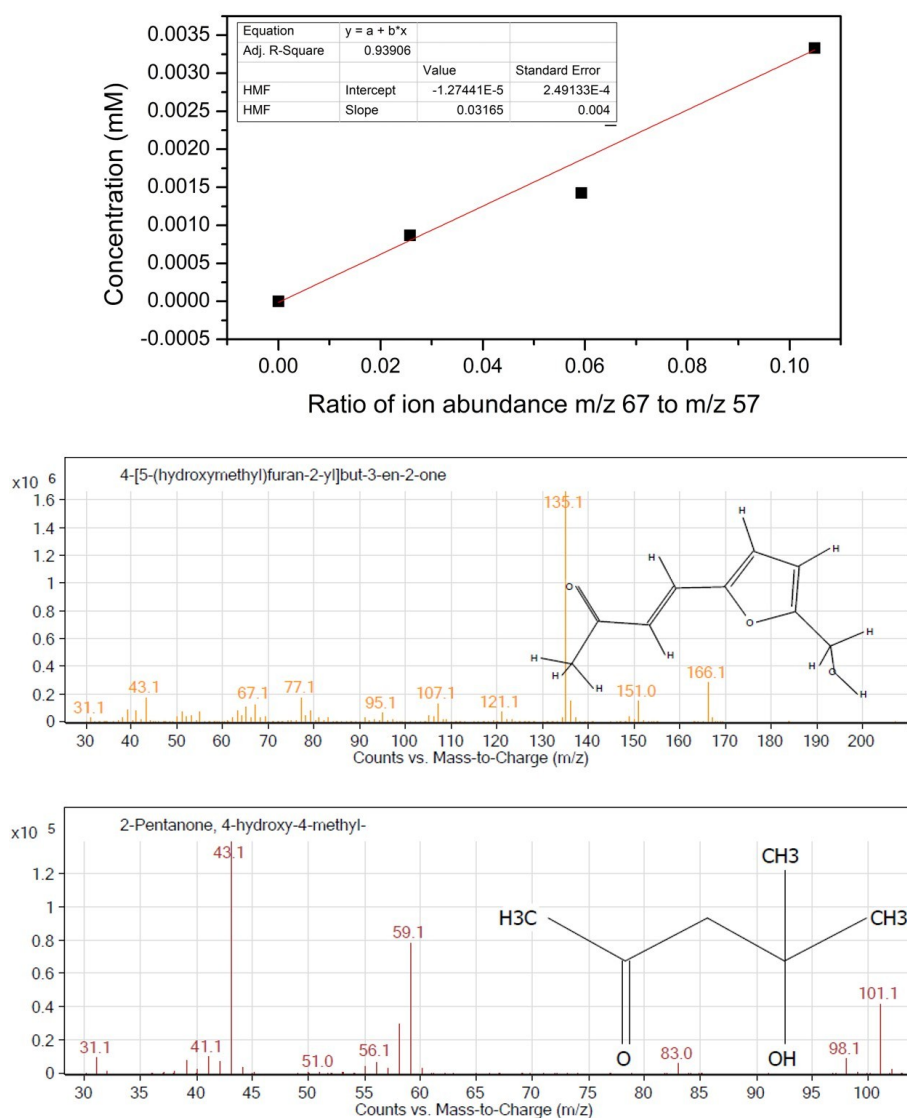


Fig. S1 Calibration curve for the ion abundance of m/z of 67 (the furan fragment ion generated from 5-HMF which is the same fragment ion found in both reactant and product) to the ion abundance of m/z of 57 (generated from decane as internal standard) and mass data spectrum corresponding to 4-[5-(hydroxymethyl)furan-2-yl]but-3-en-2-one (m/z = 166, 151, 135, 77, 43) and 4-hydroxy-4-methyl-2-Pentanone (m/z = 101, 59, 43).

In order to confirm the complete removal of all organic template, TGA-DTA analysis of as-synthesized and calcined hierarchical NaX zeolite nanosheets was performed in air in a temperature range of 100 to 1,000 °C. The TGA weight loss profile of uncalcined hierarchical NaX zeolite nanosheets (uncalcined NaX-NS) exhibits a total weight loss of ~19.9% accomplished in a two-step weight loss. The first weight loss recorded at ~196 °C was ascribed to the desorption of water inside the zeolite pores² and the second weight loss occurred at ~260 °C was ascribed to the decomposition of TPOAC template. As confirmed by the TGA weight loss profile of calcined zeolite (calcined NaX-NS), only the weight loss of adsorbed water (7.1%) was observed. Therefore, the calcination temperature of 350 °C for 15 h is efficient for complete removal of all organic templates.

Table S1. Chemical compositions analyzed by XRF of different ion-exchanged zeolites.

Samples	No. of Exchange	Composition (wt%)				Si/Al	Na/Al	%IED ^b
		SiO ₂	Al ₂ O ₃	Na ₂ O	MO ^a			
NaX-NS	-	49.7	31.5	18.5	-	1.3	1.0	-
NaX-NS-NH ₂	-	49.5	32.3	18.2	-	1.3	0.9	-
CON-NaX	-	49.6	31.8	18.5	-	1.3	1.0	-
CaX-NS	1	49.2	30.5	3.9	16.2	1.4	0.2	79.2
	2	47.8	30.9	1.8	19.3	1.3	0.1	90.5
	3	47.8	31.0	1.1	19.8	1.3	0.1	94.1
CON-CaX	3	47.5	31.9	0.8	19.6	1.3	0.0	95.7
BaX-NS	1	38.0	25.1	4.1	32.7	1.3	0.3	73.3
	2	37.1	24.1	2.5	36.1	1.3	0.2	83.1
	3	36.6	23.9	2.0	37.4	1.3	0.1	86.1
	4	36.4	23.7	1.6	38.1	1.3	0.1	88.8
	5	35.8	23.7	0.9	39.4	1.3	0.1	93.9
CON-BaX	5	34.8	24.3	0.6	40.2	1.2	0.0	95.8

^aMO=MgO, CaO, BaO ^b%IED (an ion exchange degree) = (1-(Na/Al))x100

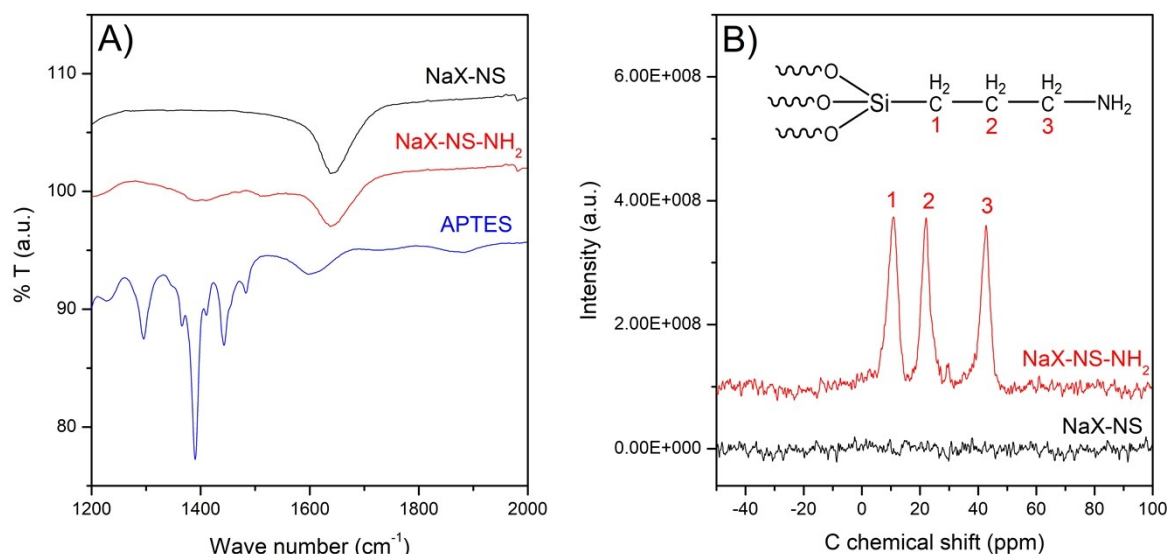


Fig. S4 A) ATR-FTIR and B) solid-state ¹³C NMR spectra of NaX zeolite nanosheets (NaX-NS, black) and amine-grafted NaX zeolite nanosheets (NaX-NS-NH₂, red).

To confirm the existence of amine group in the grafted catalysts, the ATR-FTIR and ¹³C NMR spectroscopy were used. Compared with the ATR-FTIR spectrum of non-grafted NaX zeolite nanosheets (NaX-NS, Fig. S4A), the remarkable peaks around 1399 and 1515 cm⁻¹ were observed in the case of grafted NaX zeolite nanosheets (NaX-NS-NH₂ in Fig. S4A). These peaks correspond to N-H vibration in the primary amine group (R-NH₂) in APTES.³ The ¹³C NMR spectrum of amine grafted NaX (NaX-NS-NH₂) exhibits three prominent peaks centered at 10.9, 22.2 and 42.6 ppm, which can be assigned to propyl carbon atoms in APTES as shown in Fig. S4B. These results reveal that the APTES was successfully grafted on the surface of catalysts and the organic moiety was not decomposed during the preparation procedure. In addition, it was found that all peaks corresponding to APTES disappeared in the case of non-grafted NaX zeolite nanosheets (NaX-NS, Fig. S4B), which demonstrates the absence of amine group on the unmodified zeolite. Therefore, the ATR-FTIR and ¹³C NMR experiments conclusively prove the existence of amine group on the amine grafted NaX zeolite nanosheets.

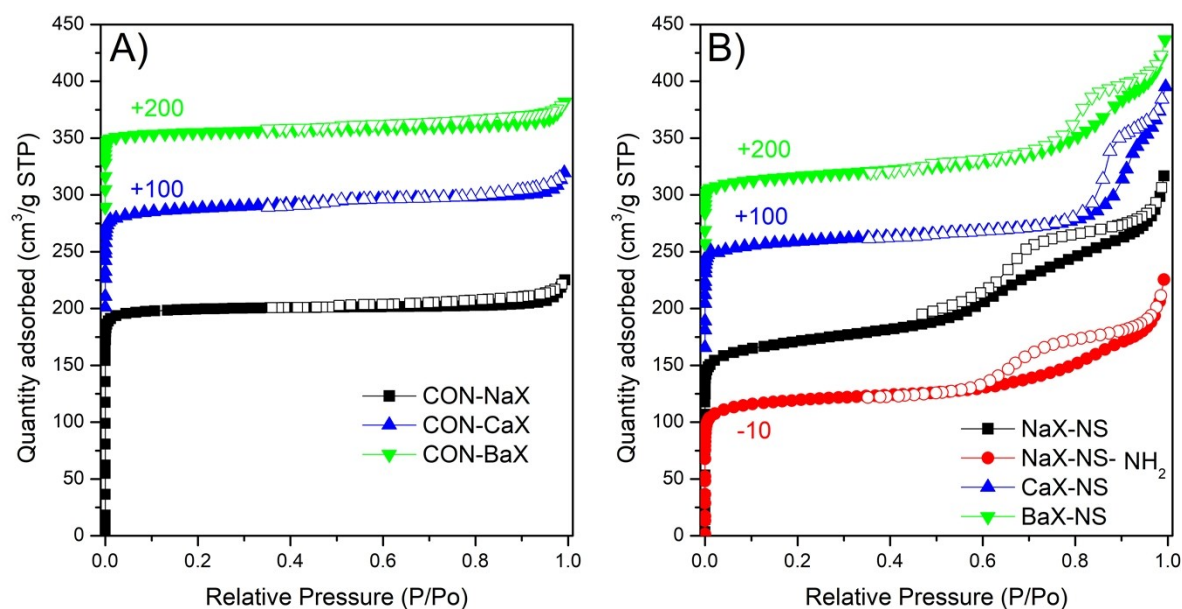


Fig. S5 N_2 adsorption-desorption isotherms of A) conventional exchanged zeolite X, and B) hierarchical zeolite X nanosheets with various alkaline cations and amine-grafting.

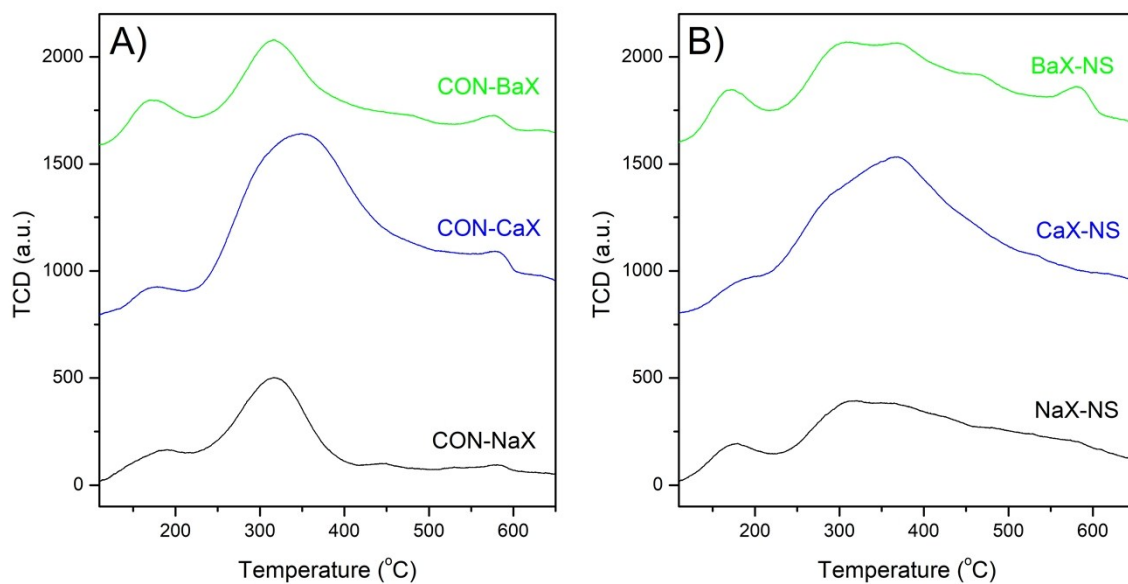


Fig. S6 CO_2 -TPD profiles of different alkali metals ion-exchanged on A) conventional zeolite X and B) hierarchical zeolite X nanosheets.

Table S2 Textural data^a, degree of crystallinity^b and total basicity^c of different alkaline metal ion-exchanged X zeolites

Sample	S _{BET} (m ² /g)	S _{micro} (m ² /g)	S _{ext} (m ² /g)	V _{total} (cm ³ /g)	V _{micro} (cm ³ /g)	V _{meso} (cm ³ /g)	Degree of crystallinity	Total Basicity ^b (mmol/g)
CON-NaX	789	719	70	0.34	0.27	0.07	85.3	0.281
CON-CaX	752	664	88	0.34	0.25	0.08	85.0	0.695
CON-BaX	634	587	47	0.28	0.22	0.06	90.5	0.256
NaX-NS	655	501	154	0.48	0.20	0.29	81.5	0.437
CaX-NS	635	531	104	0.44	0.21	0.23	77.4	0.763
BaX-NS	453	369	84	0.36	0.14	0.21	80.4	0.470
NaX-NS-NH ₂	496	377	120	0.36	0.15	0.21	73.1	n.d.
SiO ₂ -NH ₂	0.2	0.1	0.1	0	0	0	n.d.	n.d.

^a S_{BET} (BET specific surface area); S_{micro} (micropore surface area); S_{ext} (external surface area) by *t*-plot method; V_{total} (total pore volume); V_{micro} (micropore volume) by *t*-plot method. V_{ext} (external pore volume) = V_{total} - V_{micro}; The surface areas and pore volumes are in units of m²/g and cm³/g, respectively. ^b Degree of crystallinity⁴ = (total area of crystalline peaks) / (total area of all peaks) x 100%. ^c Analyzed by temperature programmed desorption of CO₂ (CO₂-TPD).

Catalytic activity

Table S3 Aldol condensation of 5-HMF and Ac at 130 °C under autogenous pressure (~6 bar) catalyzed by NaX zeolite.^a

Entry	Catalyst	Time (h)	Conv. (%)	Selectivity (%)		
				HMB	HMP	others
1	CON-NaX	6	13.97	100.00	0.00	0.00
2	CON-NaX	12	32.19	86.32	9.15	4.53
3	CON-NaX	24	32.78	89.46	5.27	5.27
4	CON-NaX	48	42.62	86.47	2.00	11.52
5	CON-NaX -2 nd run	24	32.60	91.86	5.14	3.00
6	CON-NaX -3 rd run	24	32.01	90.20	6.45	3.32
7	NaX-NS	6	18.10	92.28	3.86	3.86
8	NaX-NS	12	36.96	92.47	2.04	5.49
9	NaX-NS	24	51.03	88.53	1.82	9.65
10	NaX-NS	48	60.92	89.66	2.01	8.33
11	NaX-NS-2 nd run	24	41.86	88.88	2.39	8.73
12	NaX-NS-3 rd run	24	43.06	89.18	2.03	8.78

^aReaction condition: the amount of catalyst of 0.5g containing 10 wt.% of 5-HMF in 10 ml of acetone.

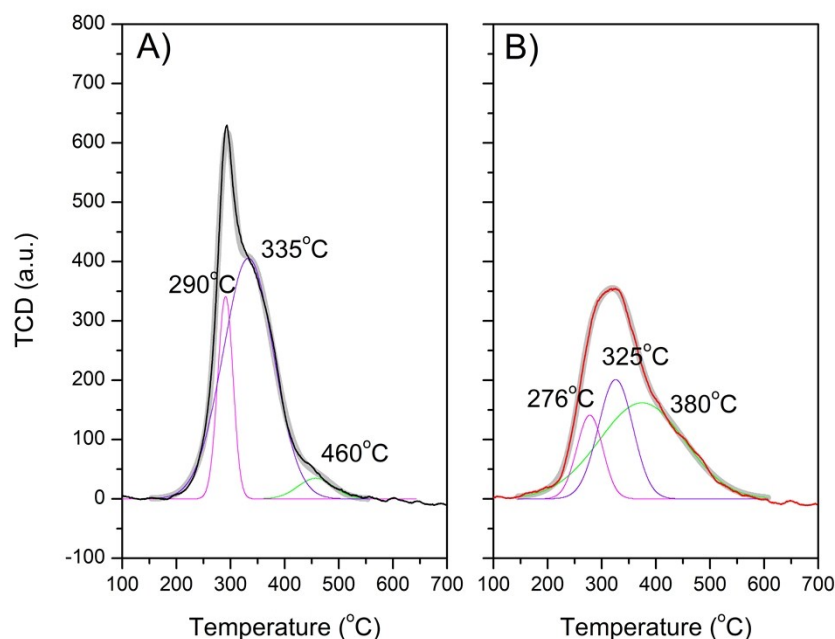


Fig. S7 Deconvoluted TPO profiles of spent catalysts A) conventional zeolite X (CON-NaX) and B) hierarchical zeolite X nanosheet (NaX-NS) obtained at the reaction time of 48 h taken at the 5-HMF conversion level of 42.62% and 60.92% for CON-NaX and NaX-NS, respectively.

The O_2 temperature programmed oxidation (O_2 -TPO) has been used for the characterization of coke species formed in zeolite structures. The deconvolution of TPO profiles exhibited three types of coke species. The peaks positioned at a low temperature ($\sim 300^\circ\text{C}$) were assigned to an easily oxidized amorphous carbon, mostly located at the outer surface of zeolite.⁵ Meanwhile, the peaks at high temperature ($\sim 400^\circ\text{C}$) indicating the higher condensation degree of cokes were assigned to graphitic carbons or the polynuclear aromatic cokes which are located inside zeolite networks.⁵ Interestingly, the shift of peak position to a lower temperature in all types of coke was observed in the case of zeolite nanosheet (NaX-NS). This result indicates that cokes formed in hierarchical structures composed of both low amorphous cokes and high condensed species and all types of coke exhibited lower degree of condensation with respect to the conventional one (CON-NaX).

Compared with the CON-NaX, the total coke content of NaX-NS obtained by integrating the area of peaks is comparable (8.49 and 7.83 mmol.g⁻¹ for CON-NaX and NaX-NS, respectively) but the ratio of high to low condensed cokes is significantly different. The great fraction of low condensed coke in CON-NaX indicates that the rapid deactivation of the catalyst is the result of pore blockage by the coke deposition on external zeolite surfaces. In contrast, the NaX-NS dramatically decreases the fraction of low condensed cokes due to the shortening of the diffusion path length. These results evidently indicate that the deactivation process of conventional zeolite was not the same as that of the nanosheet one. Besides, considering the coke formation at a comparable 5-HMF conversion level of NaX-NS (36.96%) and CON-NaX (32.78%), it was found that the NaX-NS exhibited significantly the lower coke content of 3.32 mmol.g⁻¹, while the coke content of 4.38 mmol.g⁻¹ was observed in the case of CON-NaX. These results confirm the benefits of hierarchical structures in the term of coke reduction owing to the improved mass transfer limitation.

Computational investigation

In order to clarify the properties of the 4-[5-hydroxymethyl)furan-2-yl]but-3-en-2-one (HMB) desorption on unmodified Na-exchanged zeolite X (NaX) and amine-grafted (NH₂) zeolite X (X-NH₂) systems, we performed a theoretical study using a computational chemistry approach to provide information about properties such as the adsorption energies, charge transfer, for example.

Model. The 15T quantum cluster model of faujasite zeolite (FAU) was used to present the active site of the NaX catalyst and its structure was taken from the faujasite zeolite lattice structure⁶ as shown in Fig. S8A. The dangling Si-O bonds are modified by the replacement of O atoms by the terminated H atoms at a Si-H distance of 1.47 Å in the same alignment of the corresponding Si-O bonds of the zeolite X structure. A silicon atom at T1 position of 15T active site cluster was substituted by an Al atom, leading to a negatively charge framework and it requires to neutralize by adding the H atom or cationic species. In this study, we compensated the negatively charge by Na⁺ and an amino molecule, resulting in the generation of the basic site for unmodified Na-exchanged zeolite X (NaX) and amine-grafted (NH₂) zeolite X (X-NH₂), respectively as shown in Figs. S8B and S8C. The Na⁺ cationic site located on the 6-ring of the active site, whereas the amino-grafted (NH₂) molecule was at the O2 position (see Fig. S8).

Methods. All calculations were performed using GAUSSIAN 09 code⁷ with the M06-2X density functional.⁸ Since the M06-2X method describes the van der Waals force quite well, and it has been reported that it is suitable for studying various adsorption molecules and the reaction mechanism over zeolite surfaces.⁹ The basis set of 6-31G (d,p) was employed for all atom types. During geometry optimizations, the 15T active region and the adsorbates were allowed to be relaxed while the remaining terminated hydrogen atoms were fixed at their crystallographic coordinates.

The adsorption energy (ΔE_{ads}) in the reaction was calculated by:

$$\Delta E_{\text{ads}} = E_{\text{complex}} - (E_{\text{zeolite}} + E_{\text{adsorbate}})$$

where E_{complex} is the total electronic energy of the adsorbate molecule in the zeolite X system, E_{zeolite} is the total electronic energy of the isolated zeolite X system. $E_{\text{adsorbate}}$ is the total electronic energy of the adsorbate molecule (the aldol-condensate product).

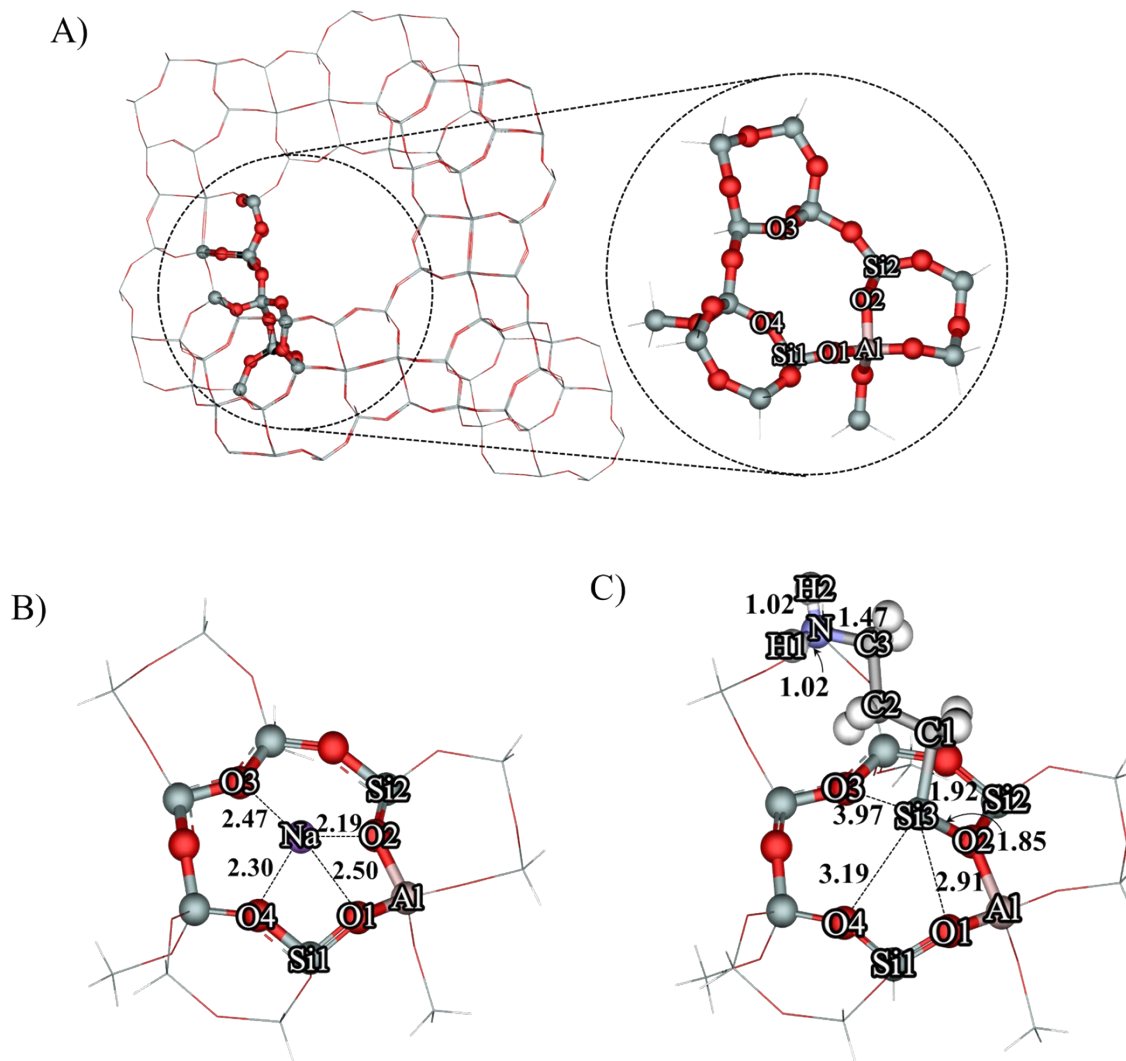


Fig. S8 Optimized structures of A) 15T quantum cluster models of zeolite X, B) the unmodified NaX, and C) the amine-grafted zeolite X.

Results and Discussion. The optimized structures and geometrical parameters of Na-exchanged zeolite X (NaX) and amine-grafted zeolite X (X-NH₂) are shown in Figs. S8B and S8C, respectively. For the Na-exchanged zeolite X (NaX), the Na⁺ was situated over the 6-ring of the active site rather close to the O2 position with the distance of 2.19 Å (Na⁺...O2) and stabilized by the interactions among the nearest O sites (O1, O3 and O4) of the active site. The partial atomic charge (Natural Population Analysis (NPA) charge) of Na was reduced from +1.000 to +0.853e. This suggests that the electron transfers from zeolite framework to Na⁺ cationic site, implying

that the zeolite framework behaves as the electron donor. The NPA charge mechanism of this work is similar to what has been described in the previous report.¹⁰ As for the amine-grafted zeolite X (X-NH₂), the NH₂-grafted molecule was coordinated with the O2 atom of the zeolite X framework via the Si3 atom with the corresponding bond distance 1.85 Å.

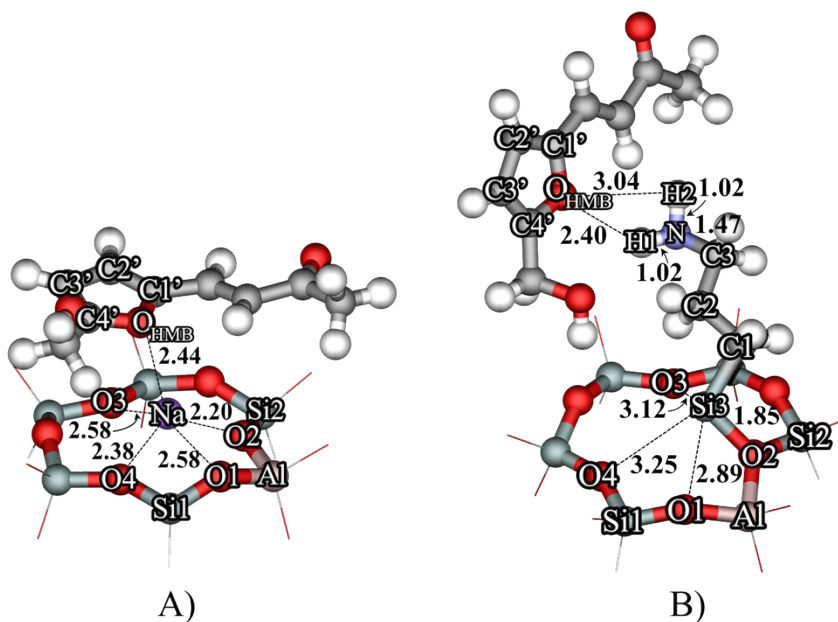


Fig. S9 Optimized structures of the adsorption configurations of HMB on A) the unmodified NaX, and B) amine-grafted zeolite X.

Figs. 9A and 9B show the optimized structures of the adsorption configurations of HMB on Na-exchanged zeolite X (NaX) and amine-grafted zeolite X (X-NH₂), respectively. For the adsorption of HMB on the NaX zeolite, the HMB molecule was adsorbed over the zeolite active site via the interactions between oxygen of HMB (O_{HMB}) and the Na site with the distance of 2.44 Å with the corresponding adsorption energy of -21.1 kcal.mol⁻¹. As for the amine-grafted zeolite X (X-NH₂), the adsorption of HMB occurred by the interactions between oxygen of HMB (O_{HMB}) and H1 of an NH₂-grafted molecule with the corresponding distance of 2.40 Å. In addition, the interaction between O_{HMB} and H2 at the bond distance of 3.04 Å could help to stabilize the adsorbed molecule in the zeolite system. The adsorption energy was reported to be -15.2 kcal.mol⁻¹, which demonstrated a weaker interaction compared to the Na-exchanged zeolite X (NaX) system by about 6 kcal.mol⁻¹. The results suggest that the HMB can be easily desorbed from the amine-grafted zeolite X (X-NH₂) system compared to that of the NaX system.

Reference

1. T. Yutthalekha, C. Wattanakit, C. Warakulwit, W. Wannapakdee, K. Rodponthukwaji, T. Witoon and J. Limtrakul, *J. Clean. Prod.*, 2017, **142**, 1244.
2. D. Xu, J. Feng and S. Che, *Dalton Trans.*, 2014, **43**, 3612.
3. X. Wang, K. S. K. Lin, J. C. C. Chan and S. Cheng, *J. Phys. Chem. B*, 2005, **109**, 1763.
4. V. Jollet, F. Chambon, F. Rataboul, A. Cabioc, C. Pinel, E. Guillon and N. Essayem, *Green Chem.*, 2009, **11**, 2052.
5. M. Ibanez, M. Gamero, J. Ruiz-Martinez, B. M. Weckhuysen, A. T. Aguayo, J. Bilbao and P. Castano, *Catal. Sci. Technol.*, 2016, **6**, 296.
6. D. H. Olson and E. Dempsey, *J. Catal.*, 1969, **13**, 221.
7. G. W. T. M. J. Frisch, H. B. Schlegel, G. E. Scuseria, M. A. Robb, J. R. Cheeseman, G. Scalmani, V. Barone, B. Mennucci, G. A. Petersson, H. Nakatsuji, M. Caricato, X. Li, H. P. Hratchian, A. F. Izmaylov, J. Bloino, G. Zheng, J. L. Sonnenberg, M. Hada, M. Ehara, K. Toyota, R. Fukuda, J. Hasegawa, M. Ishida, T. Nakajima, Y. Honda, O. Kitao, H. Nakai, T. Vreven, J. A. Montgomery, Jr., J. E. Peralta, F. Ogliaro, M. Bearpark, J. J. Heyd, E. Brothers, K. N. Kudin, V. N. Staroverov, R. Kobayashi, J. Normand, K. Raghavachari, A. Rendell, J. C. Burant, S. S. Iyengar, J. Tomasi, M. Cossi, N. Rega, J. M. Millam, M. Klene, J. E. Knox, J. B. Cross, V. Bakken, C. Adamo, J. Jaramillo, R. Gomperts, R. E. Stratmann, O. Yazyev, A. J. Austin, R. Cammi, C. Pomelli, J. W. Ochterski, R. L. Martin, K. Morokuma, V. G. Zakrzewski, G. A. Voth, P. Salvador, J. J. Dannenberg, S. Dapprich, A. D. Daniels, Ö. Farkas, J. B. Foresman, J. V. Ortiz, J. Cioslowski, and D. J. Fox, *Gaussian 09, revision c.01*, Gaussian, Inc., Pittsburgh, PA, 2009.
8. Y. Zhao and D. G. Truhlar, *Acc. Chem. Res.*, 2008, **41**, 157.
9. B. Boekfa, S. Choomwattana, P. Khongpracha and J. Limtrakul, *Langmuir*, 2009, **25**, 12990.
10. W. Sangthong, M. Probst and J. Limtrakul, *J. Mol. Struct.*, 2005, **748**, 119.